Article

Monte Carlo sampling and computational analysis of a three component tumor radiotherapy mathematical model

Md. Kamrujjaman[1], **Sayeda Irin Akter**[2], **Asma Akter Akhi**[1], **Shohel Ahmed**[3], **Mahadee Al Mobin**[1]

[1]Department of Mathematics, University of Dhaka, Dhaka-1000, Bangladesh

[2]Department of Mathematics and Statistics, York University, Toronto, ON M3J 1P3, Canada

[3]Department of Applied Mathematics, University of Alberta, AB, Canada

E-mail: kamrujjaman@du.ac.bd, irin627@yorku.ca, akhiasma752@gmail.com, shohel2@ualberta.ca, mahadeealmobin@gmail.com

Received 10 July 2023; *Accepted 5 September 2023*; *Published online 20 September 2023*; *Published 1 December 2023*

Abstract

Cancer is commonly acknowledged to be among the leading causes of death, and mathematical modeling has the potential to dramatically improve experimental cancer research. To investigate the impact of quiescent cells, we present a 3-C tumor growth model that extends the conventional Gompertz model. We used the Monte Carlo sampling technique, namely the Latin Hypercube Sampling (LHS), to determine the most critical parameters in the model dynamics. Our findings suggest that radiation therapy can be influenced by a variety of factors, including the volume of quiescent cells and the radiation sensitivity coefficient. Furthermore, in some situations, quiescent cells might transform into dividing cells, which can have a significant impact on tumor progression.

Keywords Gompertz growth; anti-angiogenetic; tumor radiotherapy; tumor volume.

Network Biology
ISSN 2220-8879
URL: http://www.iaees.org/publications/journals/nb/online-version.asp
RSS: http://www.iaees.org/publications/journals/nb/rss.xml
E-mail: networkbiology@iaees.org
Editor-in-Chief: WenJun Zhang
Publisher: International Academy of Ecology and Environmental Sciences

1 Introduction

If we try to find the prime causes of death worldwide, cancer would be one of them. Although our medical fields have been improved a lot, some cancers are hard to overcome, for example, lung cancer (Jemal et al., 2011a; Ferlay et al., 2015a). According to the data, there were approximately 14.1 million new instances of cancer and 8.2 deaths associated with cancer globally during the year 2012. Using mathematics, we can contribute to many areas of experimental cancer investigation and explore the aspect of cancer; different mathematical models have been introduced so far (Kim et al., 2007a; Cristini, 2009a; Deisboeck and Stamatakos, 2010a; Ira et al., 2020a; Kamrujjaman et al., 2021a; Kim et al., 2011b). Mathematical modeling can be a potential tool to analyze the dynamics of complex systems and experiment hypotheses. Clinical data could be used to calibrate the model (Wang et al., 2009b; Macklin et al., 2012a; Hossine et al., 2019a; Gao et

al., 2013a), and competing hypotheses of tumorigenesis and therapy alternatives could be investigated prior to starting clinical treatment (Rockne et al., 2010b; Enderling et al., 2007b; Cappuccio, 2006; Marcu et al., 2009c; Powathil et al., 2012b).

Different techniques are used for treating a cancer patient, including surgical procedures, radiation therapy, and chemotherapy. Recently the application of radiation therapy for cancer management has become a major interest to many investigators who use mathematical modeling to find the result. Rigorous investigations have been done on cancer progression and its response to radiation therapy. Both stochastic models and significant biological processes such as apoptosis and angiogenesis at the molecular level were used (Borkenstein et al., 2004a; Harting et al., 2007c; Titz and Jeraj, 2008a; Alam et al., 2020b). The reference articles (Rockne et al, 2009d; Perez-Garcia et al., 2014a; Nawrocki and Zubik-Kowal, 2014b) represented tumor growth as diffusion in three-dimensional space, applying the model to investigate the progression of cancer and its response to radiation therapy focusing on glioblastoma multiforme (GBM) and low-grade glioma, which are brain tumors. Cancer metabolic process is very complex, and the mechanism is still yet to be discovered. Scientists have been trying since the early 1900s when mathematical modeling was projected to conduct clinical treatment to treat cancer which has got a new dimension due to the extensive improvement in computer science technology (Bratus et al., 2014c; Nazila and Lotfi, 2016a).

The uncontrolled multiplication of the cell leads to the emergence of cancer. Cancer cells proliferate abnormally, affect the normal cells in the body, and eventually spread to the whole body without responding adequately to the system controlling the healthy cell response. Since cancer could be raised due to abnormal proliferation of any type of cells, as a result, there are over a hundred different forms of cancer, each with its unique characteristics and clinical intervention. The most critical topic in cancer pathophysiology is the difference between benign and malignant tumors. A benign tumor is limited to its site of origin not infecting the nearby cells while the malignant one has the capability to infect healthy cells and spread to other organs, which is done by the circulatory or lymphatic systems known as metastasis (Cooper et al., 2007d).

Cancer-inducing substances are known as carcinogens. Multiple complicated steps are required to develop cancer, and many factors are responsible for this. A commonly accepted argument is that mutation of the gene is responsible for turning a healthy cell into cancer cells despite having several controversies regarding the initialization of cancer (Michor et al., 2004b). However, other substances cause cancer by accelerating the proliferation of cells known as tumor promoters. A basic difference between a cancer cell and a normal cell is that the normal cell exhibits density-dependent inhibition (DDI) in cell multiplication, meaning the normal cell continues to be proliferated to reach a specific density level. On the other hand, cancer cells are insensitive to the DDI (Cooper et al., 2007d).

In this study, we have considered two different models: first, the tumor growth model and its corresponding dynamics, while in the second phase, we designed a model to reduce the tumor volume by treatment strategy using multiple factors. The results suggest that various factors, including the volume of quiescent cells and the radiation sensitivity coefficient, can influence radiation therapy. Moreover, in many cases, quiescent cells might transform into dividing cells, which can significantly impact tumor progression.

The article is organized as follows: a three-component mathematical model of tumor growth is discussed elaborately in Section 2 with a flow diagram and established theoretical results. Section 3 discussed the inducing cell death in proliferative tumor cells or lowering tumor support to reduce tumor size significantly. The Latin Hypercube Sampling, scheme, and heat maps are presented in Section 4. Section 5 features computational results to visualize the tumor size upward and reduce the volume size. Finally, the results are summarized in Section 6.

2 Three-component (3-C) Mathematical Model

Researchers sometimes classify malignant cells into two different categories: dividing and non-dividing cells, where the growth of the tumor depends on the first one, and the non-diving cells will be eliminated from the body once they are dead. This type of model is known as the two-component (2-C) Model (Yoichi et al., 2016b; Chvetsov et al., 2009e). Although the quiescent cells are overlooked here, this type of cell has a crucial role in tumor progression. It is observed that the environment filled with nutrients is conducive for malignant cells to proliferate. On the other hand, programmed cell death, known as apoptosis, happens when the nutrient level is low while the tumor cells remain quiescent when the nutrient level is medium. Sometimes dividing cells may arise from the quiescent cells that can affect the growth of tumor cells, although special circumstances are required for this event. A mathematical model regarding nutrient ingestion and diffusion within malignant cells has been proposed since the mid of 1960s. Several evaluations of this topic of tumor modeling have been published in recent years (Araujo and McElwain, 2004c; Adam, 1996; Byrne, 1999a). In fact, nutrient (in particular oxygen) diffusion limits tumor spheroid growth, leading to the angiogenesis hypothesis. According to this theory, tumors should have their blood arteries become large; hence they must acquire vessels from the host vasculature via angiogenesis (Carmeliet and Jain, 2000). This theory has prompted extensive study into a possible cancer cure based on the identification of substances that inhibit angiogenesis (Blagosklonny, 2004d). For more actual analysis, a 3-C model is proposed in this paper. The ODE model is given by the following

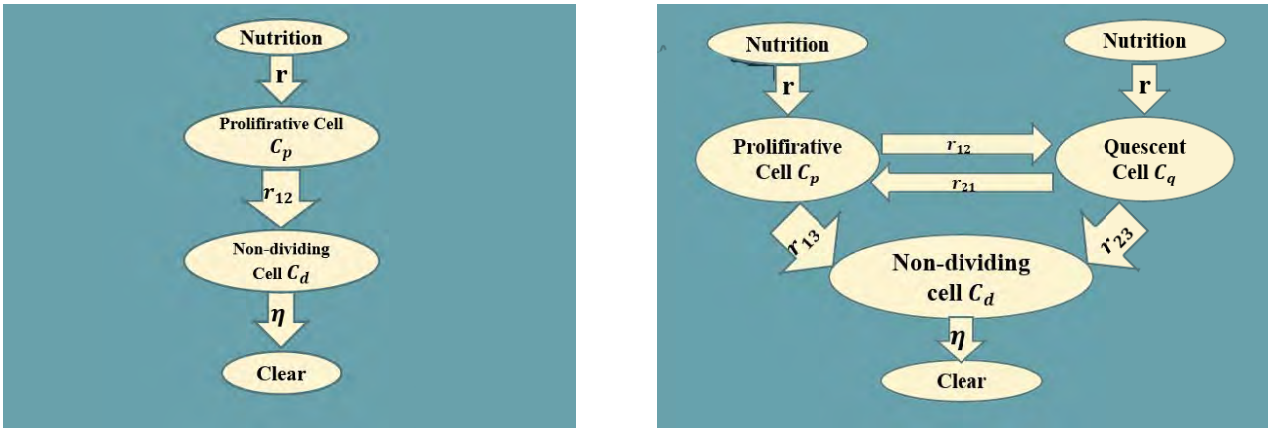

Fig. 1 (Left) 2-Component model; (right) 3-Component model.

$$\begin{cases} \dfrac{dC_p}{dt} = \mu C_p - \lambda C_p \ln\left(\dfrac{C_p}{K}\right) - (r_{12} + r_{13})C_p + r_{21}C_q + r \\ \dfrac{dC_q}{dt} = r_{12}C_p + r - (r_{21} + r_{23})C_q \\ \dfrac{dC_d}{dt} = r_{13}C_p + r_{23}C_q - \eta C_d \end{cases} \tag{2.1}$$

where C_p is the proliferative (dividing) cell volume, C_q is the quiescent cell volume, C_d is the dead or non-dividing cell volume, r_{ij} is the rate of change from state i to state j, η is the cell clear rate and the fresh nutrient provided by the vasculature with rate r.

Lemma 1. The dynamic (2.1) preserves positivity.

$$C_p^0 > 0, C_q^0 > 0, C_d^0 > 0 \Rightarrow C_p(t) > 0, C_q(t) > 0, C_d(t) > 0, \ \forall t > 0 \tag{2.2}$$

Proof. We define, $z(t) = \frac{1}{2}\left[C_p(t)_-^2 + C_q(t)_-^2 + C_d(t)_-^2\right]$ and note that $z(0) = 0$. Using the chain rule we compute

$$\begin{aligned}
\dot{z}(t) \quad &= -C_{p-}\dot{C}_p - C_{q-}\dot{C}_q - C_{d-}\dot{C}_d \\
&= -C_{p-}\left[\mu C_p - \lambda C_p \ln\left(\frac{C_p}{K}\right) - (r_{12} + r_{13})C_p + r_{21}C_q + r\right] \\
&-C_{q-}\left[r_{12}C_p + r - (r_{21} + r_{23})C_q\right] - C_{d-}\left[r_{13}C_p + r_{23}C_q - \eta C_d\right] \\
&\leq \mu C_{p-}^2 - r\left(C_{p-} + C_{q-}\right) + (r_{12} + r_{21})C_{p-}C_{q-} + r_{13}C_{p-}C_{d-} + r_{23}C_{q-}C_{d-}
\end{aligned}$$

Because terms as $C_{p-}C_p = -C_{p-}^2$ or $-C_{p-}C_{q+}$ are non-positive. Therefore, we conclude that, for some constant $\gamma > 0$,

$$\dot{z}(t) \leq \gamma\left[C_p(t)_-^2 + C_q(t)_-^2 + C_d(t)_-^2\right] = \gamma z(t)^2$$

Because $z(0) = 0$ and $z(t) \geq 0$, we conclude that $z(t) \equiv 0$.

Lemma 2. The dynamic (2.1) is a "monotonic operator" i.e.

$$\begin{aligned}
&\dot{C}_p(0) > 0, \dot{C}_q(0) > 0, \dot{C}_d(0) > 0 \\
&\Rightarrow \dot{C}_p(t) > 0, \dot{C}_q(t) > 0, \dot{C}_d(t) > 0 \quad \forall t > 0
\end{aligned} \tag{2.3}$$

Proof. Suppose,

$$\begin{aligned}
\alpha(t) \quad &= \dot{C}_p(t) \\
\beta(t) \quad &= \dot{C}_q(t) \\
\zeta(t) \quad &= \dot{C}_d(t)
\end{aligned}$$

Differentiating equations (2.1) gives

$$\begin{cases}
\dot{\alpha}(t) = F(C_p)\alpha - (r_{12} + r_{13})\alpha + r_{21}\beta + r, \ \left[F(C_p) = \mu - \lambda K - \lambda \ln\left(\frac{C_p}{K}\right)\right]. \\
\dot{\beta}(t) = r_{12}\alpha + r - (r_{21} + r_{23})\beta \\
\dot{\zeta}(t) = r_{13}\alpha + r_{23}\beta - \eta\zeta
\end{cases} \tag{2.4}$$

Deducing based on the signs of $\alpha(t), \beta(t)$ and $\zeta(t)$ we compute

$$\begin{aligned}
&\frac{1}{2}\frac{d}{dt}[\alpha(t)_-^2 + \beta(t)_-^2 + \zeta(t)_-^2] \\
&= \left[F'(C_p) - (r_{12} + r_{13})\right]\alpha(t)_-^2 - r_{21}\beta\alpha(t)_- - r_{12}\alpha\beta(t)_- - r_{13}\alpha\zeta(t)_- - r_{23}\beta\zeta(t)_- \\
&-r(u(t)_- + v(t)_-) - (r_{21} + r_{23})v(t)_-^2 - \eta w(t)_-^2 \\
&\leq \left[\left|F'(C_p) - (r_{12} + r_{13})\right| + \frac{r_{12} + r_{21} + r_{13} + r_{23}}{2} + (r_{21} + r_{23} + \eta)\right][\alpha(t)_-^2 + \beta(t)_-^2 + \zeta(t)_-^2]
\end{aligned}$$

Because $\alpha(0)_-^2 + \beta(0)_-^2 + \zeta(0)_-^2 = 0$, we deduce that $\alpha(t)_-^2 + \beta(t)_-^2 + \zeta(t)_-^2 \equiv 0$.

Lemma 3. ((Elisabet), Lemma 1.6) The non-trivial steady state is linearly stable for small death rate i.e.

$(r_{13} + r_{23})$ being very small.

$$\overline{C_p} = C_{p0}K,\ C_{p0} = \mu - \lambda \ln\left[\frac{\lambda(r + r_{21} + r_{13} + r23 + \eta)}{(r + r_{12} + r_{13})(\eta + r_{13} + r_{23})}\right]$$
$$\overline{C_q} = \left[\frac{r + r_{12} + r_{13}}{r + r_{21} + r_{13} + r_{23} + \eta}\right]\overline{C_p} \tag{2.5}$$

The zero steady state $(0,0)$ is linearly unstable if $\frac{\lambda}{\mu} > (r + r_{12} + r_{13})$.

The following theorem is a detailed mathematical conclusion regarding the system of ordinary differential equations concerning proliferative, quiescent, and dead cells.

Theorem 1. ((Elisabet), Theorem 1.8) We assume death rate of cells is zero, that is $(r_{13} + r_{23}) = 0$. For $C_p(0) \geq 0, C_q(0) \geq 0, C_d(0) \geq 0$ and $\big(C_p(0), C_q(0), C_d(0)\big) \neq (0,0,0)$ the solution of system (2.1) satisfies that

$$C_p(t) \quad \to K,\ t \to \infty,$$
$$C_q(t) \quad \to \left[\frac{r + r_{12} + r_{13}}{r + r_{21}}\right]K,\ t \to \infty.$$

We can also extend the theorem for non-zero death rate $(r_{13} + r_{23}) > 0$.

3 Radiotherapy 3-C Mathematical Model

Nutrients like oxygen, glucose cannot enter inside the tumor cell once it has grown to a diameter of about 1 mm which causes cell death known as necrosis. Then the Vascular Endothelial Growth Factors (VEGF) are released by necrotic cells, causing neovasculature to form. Nutrients can thus be delivered in greater quantities to the tumor which helps the cells to be developed again. The concept of employing anti-angiogenetic (AA) medications to inhibit tumor progression dates back to the 1970s (Folkman, 1972). Bevacizumab, a monoclonal antibody, was developed in 2004. (Commercial name: Avastin) has been shown to have anti-tumor activity, however, it is usually used in conjunction with chemotherapeutic drugs. Several studies have come to differing outcomes AA may be effective on primary cancers by accelerating metastatic tumors, AA scheduling, and cytotoxic medicines may have a major role). Several considerations are possible: decreasing the vasculature causes the limited chemotherapeutic delivery towards the malignant cells. Recently it has been revealed that instead of decreasing vasculature, AA normalizes it.

Tumors can be treated using one of two methods. Inducing cell death in proliferative tumor cells or lowering tumor support via reduced carrying capability can both result in a significant reduction in tumor size. Differential equation models can easily incorporate the impacts of both types of cancer therapy (Hahnfeldt et al., 1999b):

$$\frac{dn}{dt} = \mu n - \lambda n \ln\left(\frac{n}{K}\right) - \xi n$$
$$\frac{dK}{dt} = \phi n - \varphi K n^{2/3} - \vartheta K g(t)$$

Here,

- ϕ is the angiogenesis rate. It is positive, invariant by supposition.
- φ is the inhibition rate. It is positive, invariant by supposition.

- $\xi \in [0,1]$ is the strength of annihilation of a continuous tumor cell by the anti tumor treatment of discussion, preferably immunotherapy or chemotherapy.

According to Hahnfeldt et al. (1999b), the diminution of angiogenesis caused by governed antiangiogenic medications is proportional to the dose concentration $g(t)$, which includes partially cleared concentration of the previous dose.

$$g(t) = \int_0^{\infty} \Lambda(t')e^{-\Psi(t-t')}dt'$$

Here,

- $\Lambda(t')$ is the administration rate of inhibition concentration.
- $\Psi(t-t')$ is the clearance rate of inhibition concentration.

The interaction between radiation rays and tumor cells in radiotherapy is quite diverse due to the different properties. The usual model for radiation-induced cell death after a single dose supposes that some tumor cells die while the rest continue to proliferate. The LQ model is the most prevalent and widely utilized for X-ray or gamma-ray (Matthias et al., 2013b; Masahiro et al., 2012c). Its formulation in terms of ordinary differential equation is as follows

$$\frac{dC}{dt} = -(\gamma R_d + 2\delta R_d^2)C \tag{3.1}$$

Here,

- C is the volume of the tumor.
- R_d is the dose of radiation.
- γ is the coefficient of the linear item.
- δ is the coefficient of the quadratic item.

Normally, γ/δ depicts the radiation sensitivity of the tumor cells. It is widely known that, tumor cells in different phases are more or less sensitive to radiation. Hence, this article assumes that radiation beams only affect on proliferating and quiescent cells with varying sensitivity. The system of ordinary differential equations modelling this phenomenon is as follows:

$$\begin{cases} \frac{dC_p}{dt} = \mu C_p - \lambda C_p \ln\left(\frac{C_p}{K}\right) - (r_{12} + r_{13})C_p + r_{21}C_q + r - (\gamma_1 R_d + 2\delta_1 R_d^2)C_p \\ \frac{dC_q}{dt} = r_{12}C_p + r - (r_{21} + r_{23})C_q - (\gamma_2 R_d + 2\delta_2 R_d^2)C_q \\ \frac{dC_d}{dt} = r_{13}C_p + r_{23}C_q - \eta C_d \end{cases} \tag{3.2}$$

where $\gamma_1, \delta_1; \gamma_2, \delta_2$ are the radiation sensitivity of quiescent cells and dividing cells, respectively. In regular radiotherapy, fractional radiotherapy is now the prevalent plan. It is crucial to assess tumor cell proliferation as well as changes in quiescent cells between two fractions. The model described is hence unsuitable for simulating the process. We thus propose a piecewise integration model for fractional radiotherapy simulation in this paper:

$$C_p = \sum_{i=1}^{N} \left(\int_0^{t_*} - \left(\gamma_1 R_{di} + 2\delta_1 R_{di}^2\right) C_{pi} dt \right) + \sum_{i=1}^{N} \left(\int_{t_0}^{t_d} \left(\mu C_{pi} - \lambda C_{pi} \ln\left(\frac{C_{pi}}{K(i)}\right) - (r_{12} + r_{13}) C_{pi} + r_{21} C_{qi} + r \right) dt \right) \quad (3.3)$$

Here,

- R_{di} is the dose of radiation in each fraction.
- $(0, t_*)$ is the time length of the radiation.
- (t_0, t_d) is the time lapse between two fractions.
- C_{pi} is the volume of C_p at i^{th} fraction.
- C_{qi} is the volume of C_q at i^{th} fraction.
- N is the total number of radiotherapy fractions.

We can construct the integration model for C_q in a similar fashion.

$$C_q = \sum_{i=1}^{N} \left(\int_0^{t_*} - \left(\gamma_2 R_{di} + 2\delta_2 R_{di}^2\right) C_{qi} dt \right) + \sum_{i=1}^{N} \left(\int_{t_0}^{t_d} \left(r_{12} C_{pi} + r - (r_{21} + r_{23}) C_{qi} \right) dt \right) \quad (3.4)$$

4 Sensitivity Analysis

This article performed a sensitivity analysis to test the model's (2.1) robustness to parameter values, which aids the identification of the most crucial parameters in model dynamics. The Latin Hypercube Sampling (LHS) scheme is utilized for parameter estimation that samples over numerous values over the topological space of the parameters to be estimated as described in Table 1 (Marino et al., 2008b). 5000 model simulations were run for the system of differential equations presented in by randomly selecting paired sampled values for all LHS parameters as described in (2.1). Fig. 2 depicts the corresponding non-linear yet unmodulated interaction among model state variables and each parameter using Partial Rank Correlation Coefficients (PRCC) and p-values. Furthermore, if the associated p-value is smaller than 1%, the output is considered statistically significant.

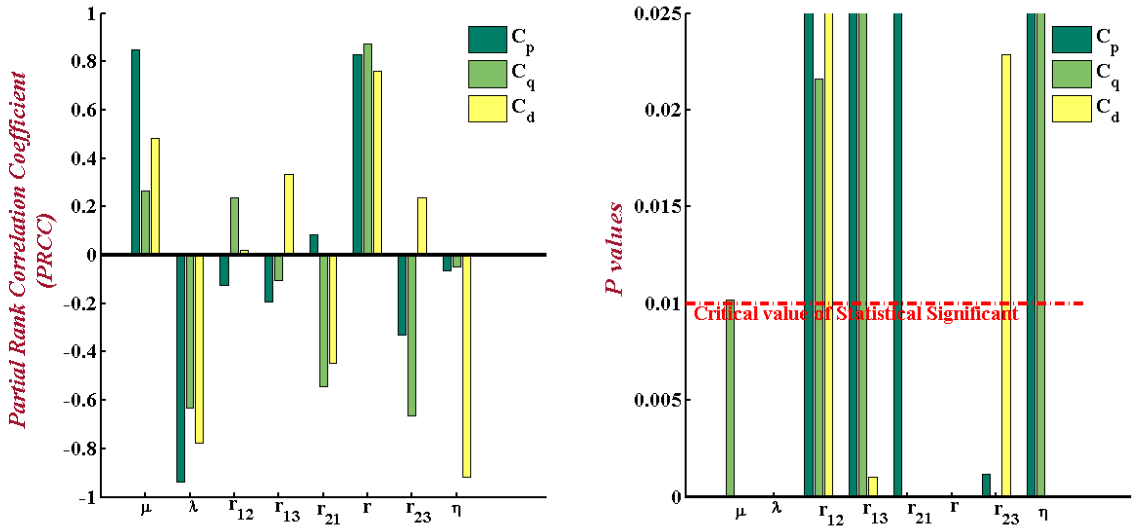

Fig. 2 PRCC values for the 3-C model (2.1).

Fig. 2 illustrates, μ, λ, r_{21}, r, and r_{23} to be the parameters those strongly influence the dynamics of tumor growth. Parameters μ and r have a positive influence; i.e. deviation of parameter is directly proportinal to the model variables. While parameter λ negatively influences the model compartments, other significant parameters have a mixed influence on the model variables. Another significant result is shown in the following Fig. 3 generated by utilizing the Perturbation Theory Toolbox for Systems (PeTTSy) (Domijan et al., 2016c), which illustrates the sensitivity heat map (SHM) of the model variables concerning time, corresponding to the model parameters. This is because the variable C_q (quiescent cell volume) is the most sensitive model variable to all factors throughout the simulation period, followed by C_p (proliferative cell volume) and C_d (dead cell volume).

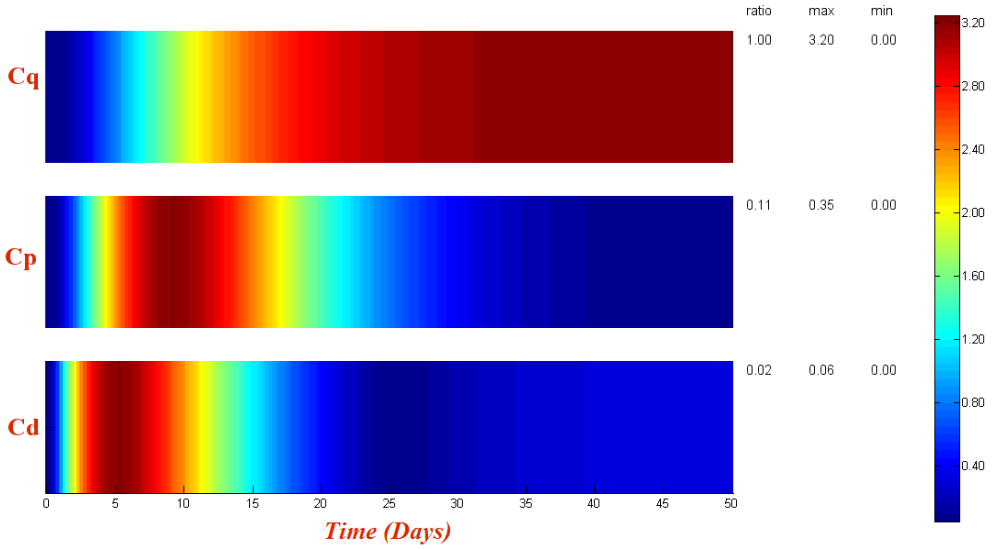

Fig. 3 Heat diagram of parameter and model variable sensitivity with maximum value 3.2017.

Thus, sensitivity analysis helps to conclude that in order to curtail the factors for tumor growth such as (recruitment rate (μ), and Nutrition Rate (r)), we need to amplify some therapeutic treatment strategies on the important compartment C_p and C_q.

5 Results and Discussion

This section features the topological nature of the model (3.2) under different parameters settings. Parameter values are given in Table 1. For illustration, this article the value of the parameters to be assumed within actual limit for a typical scenario in a human body.

Table 1 Description of parameter values used in the model (2.1).

Notation	Interpretation	Values/Range	References

μ	Recruitment rate	$0.005 - 0.2$	Estimated
λ	Gompertz growth rate	$0.25 - 1.50$	Estimated
r_{12}	Rate of transition from Proliferative cell to Quiescent cell	$0.05 - 0.15$	Estimated (Wen-song and Gang-qing, 2019b)
r_{21}	Rate of transition from Quiescent cell to Proliferative cell	$0.05 - 0.15$	Estimated (Wen-song and Gang-qing, 2019b)
r_{13}	Rate of transition from Proliferative cell to Non-dividing cell	$0.04 - 0.06$	Estimated (Wen-song and Gang-qing, 2019b)
r_{23}	Rate of transition from Quiescent cell to Non-dividing cell	$0.04 - 0.06$	Estimated (Wen-song and Gang-qing, 2019b)
r	Nutrition Rate	$0.50 - 2.50$	Estimated
η	Cell clearance rate	$0.05 - 0.35$	Estimated (Wen-song and Gang-qing, 2019b)

5.1 Model calibration without radiotherapy

Simulation and analysis for tumor growth model

Example 1. (effect of λ) We consider Equation (2.1) with $= 0.005, r_{12} = r_{21} = 0.1, r_{13} = r_{23} = 0.05, \eta = 0.2$. We take here $K = 1.0$, a constant and $K = 1.2 + \cos(\pi t)$. We change here the Gompertz growth rate by 50 percent and 75 percent $\lambda = 0.25, 0.75, 1.50$ and observe the behavior of the tumor volume in Fig. 4.

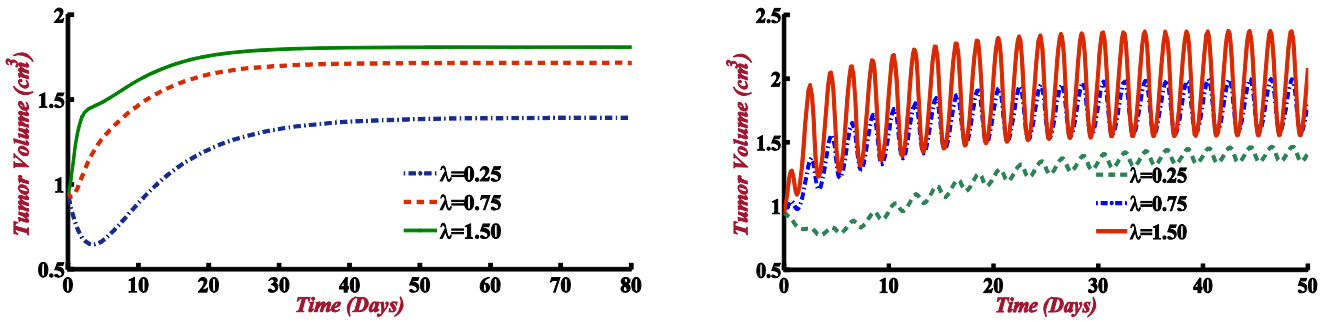

Fig. 4 Total tumor volume of (2.1) for different Growth rate λ; (left) for $K = 1.0$; (right) for $K = 1.2 + \cos(\pi t)$.

Example 2. (effect of μ) We consider Equation (2.1) with $r_{12} = r_{21} = 0.1, r_{13} = r_{23} = 0.05, \eta = 0.2$. We take here $K = 1.0$. We have changed recruitment rate $\mu = 0.005, 0.01, 0.02$ and observe the behavior of the tumor volume in Fig. 5.

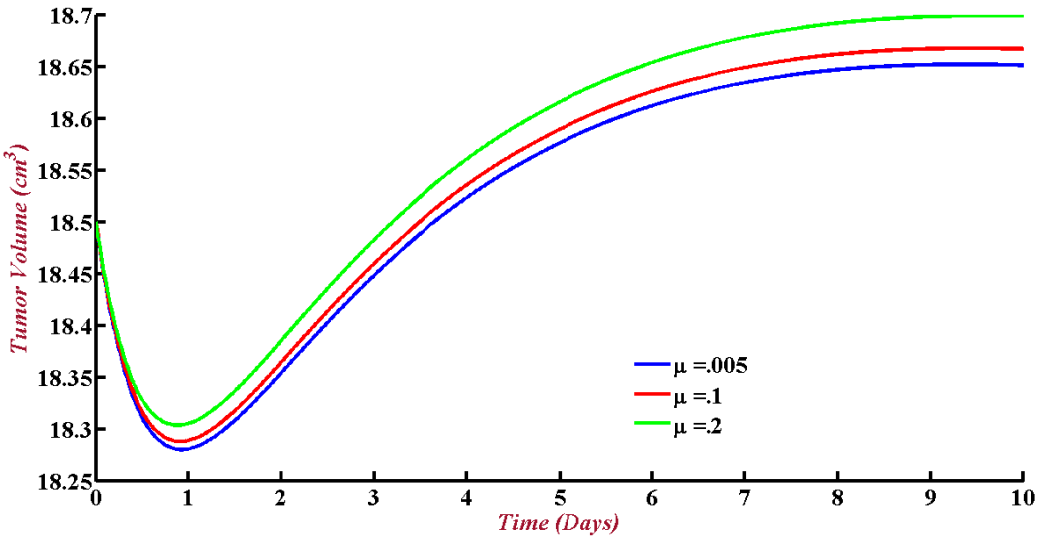

Fig. 5 Total tumor volume of (2.1) for different recruitment rate μ.

Example 3. (Overall effect of r_{12} and r_{21}) We consider Equation (2.1) with $= 0.005, \lambda = 0.75, r_{21} = 0.1, r_{13} = r_{23} = 0.05, \eta = 0.2$. We take here $K = 1.0$, a constant. We know that the rate of proliferative cell to quiescent cell r_{12} increase with the decrease of nutrition. That is, with high nutritions the proliferative cells convert to the quiescent cells in a very low rate and with low nutritions the proliferative cells convert to the quiescent cells in a very high rate. We take $r_{12} = 0.05, 0.10, 0.15$ to observe the behavior (Fig. 6).

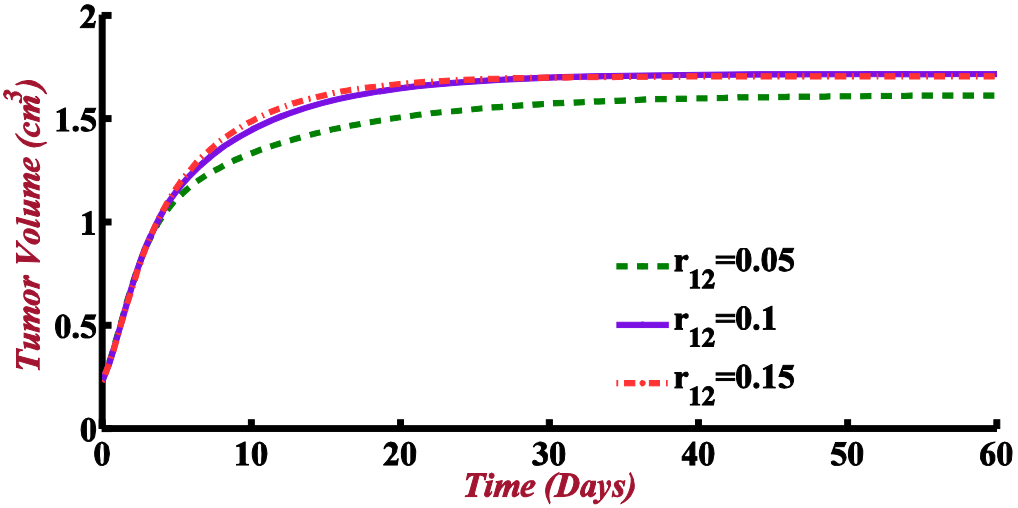

Fig. 6 Total tumor volume of (2.1) with the of change r_{12}.

Similarly, we observe the change while rate of change from quiescent cells to proliferative cells $r_{21} = 0.15, 0.1, 0.05$. Here the quiescent cells convert to the proliferative cells in a high rate with a high nutrition environment (Fig. 7).

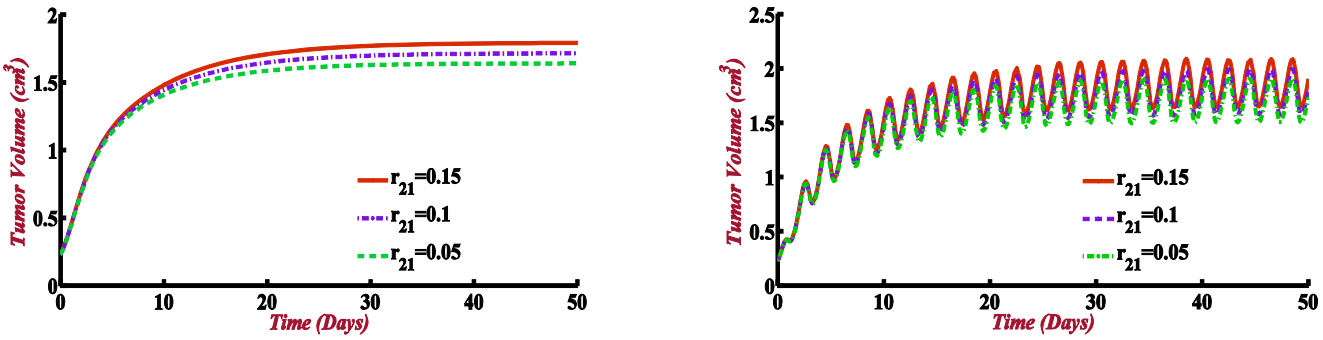

Fig. 7 Total tumor volume of (2.1) for different nutrition rate with the of change r_{21} (left) for $K = 1.0$; (right) for $K = 1.2 + \cos(\pi t)$.

Example 4. (Overall effect of r_{13} and r_{23}) We consider Equation (2.1) with $= 0.005, \lambda = 0.75, r_{12} = r_{21} = 0.1, \eta = 0.2$. We take here $K = 1.0$, a constant. We know that the rate of the proliferative cell to dead cells r_{13} increases with the decrease in nutrition. With high nutrition, the proliferative cells convert at a very low rate to the dead cells, and with low nutrition, the proliferative cells convert to the dead cells at a high rate. This is also the same for converting quiescent cells to dead cells. We take $r_{13} = r_{23} = 0.05, 0.10, 0.15$ and observe the behavior of total tumor volume (Fig. 8).

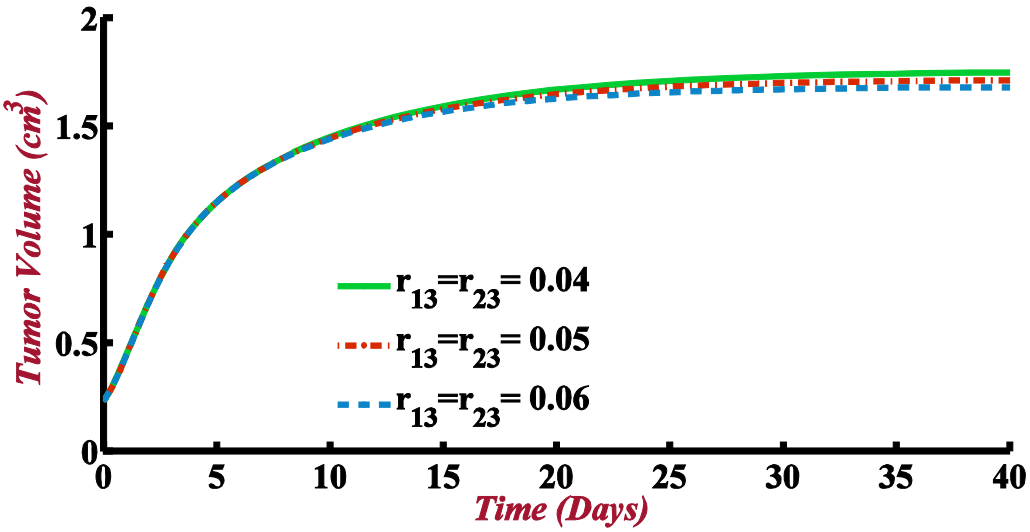

Fig. 8 Total tumor volume of (2.1) with the of change of r_{13} and r_{23}.

Example 5. (Overall effect of η) We consider Equation (2.1) with $= 0.005, \lambda = 0.75, r_{12} = r_{21} = 0.1, r_{13} = r_{23} = 0.05$. We take here $K = 1.0$, a constant. We change the clearance rate by 75 percent as $\eta = 0.05, 0.2, 0.35$ and observe the behavior of the total tumor volume, see Fig. 9.

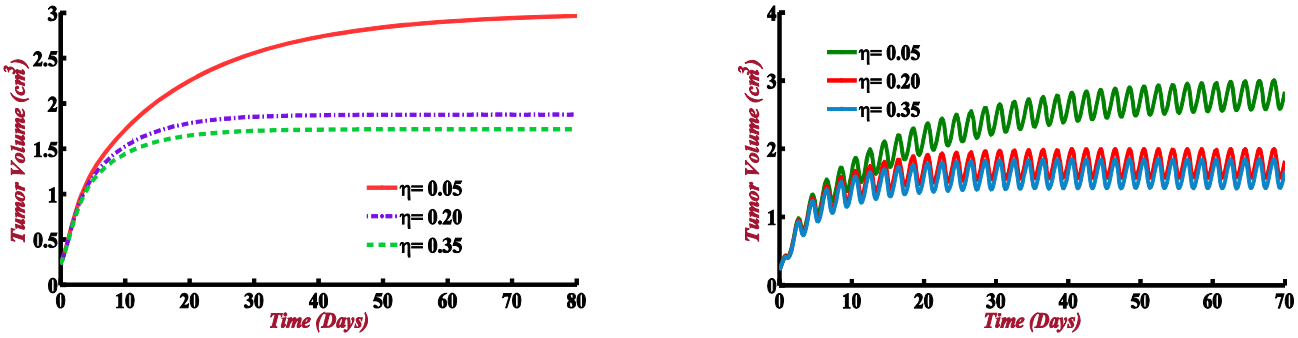

Fig. 9 Total tumor volume of (2.1) for different clearance rate η (left) for $K = 1.0$; (right) for $K = 1.2 + \cos(\pi t)$.

5.2 Model calibration with radiotherapy

In general, the higher the dose (fractional/continuous), the better the tumor control and the faster the model convergence. Of course, a bigger dose will injure the normal tissues around it. To optimize tumor radiotherapy, the radiation models for normal tissues and those for the tumor must be considered.

Example 6. (Impact of fractional dose) We consider Equation (3.2) with $\mu = 0.005, \lambda = 0.75, r_{12} = 0.1, r_{21} = 0.1$, $r_{13} = r_{23} = 0.05$. We take here $K = 1.2 + \cos(\pi t), \eta = 0.3, \gamma_1 = 1.5, \delta_1 = 0.125, \gamma_2 = 2.1, \delta_2 = 0.51$. We change the fractional dose R_d and observe the behavior of the total tumor volume.

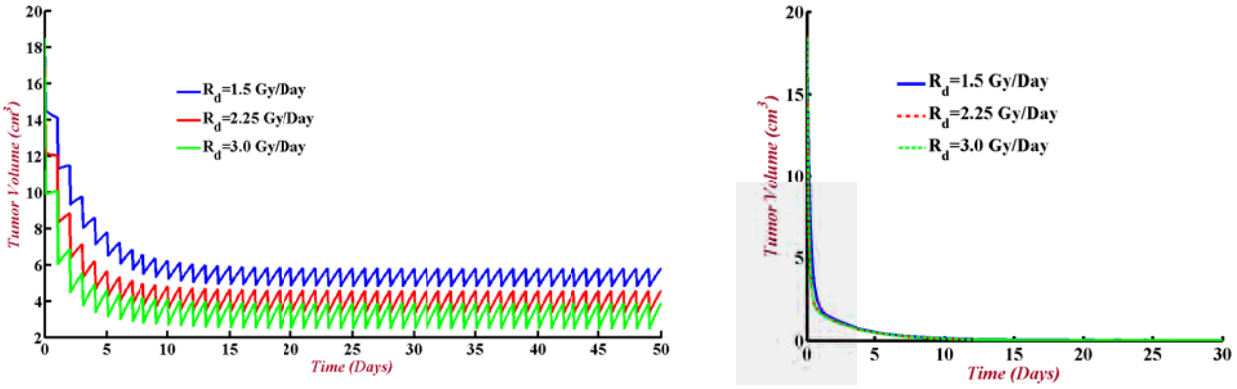

Fig. 10 Total tumor volume of (3.2) for constant $r = 1.5$ (left), and $r = 0$ (right).

Example 7. (Impact of Continuous dose) We consider Equation (3.2) with $= 0.005, \lambda = 0.75, r_{12} = 0.1, r_{21} = 0.1, r_{13} = r_{23} = 0.05$. We take here $K = 1.2 + \cos(\pi t), \eta = 0.3, \gamma_1 = 1.5, \delta_1 = 0.125, \gamma_2 = 2.1, \delta_2 = 0.51$. We change the radiotherapy dose R_d and observe the behavior of the total tumor volume.

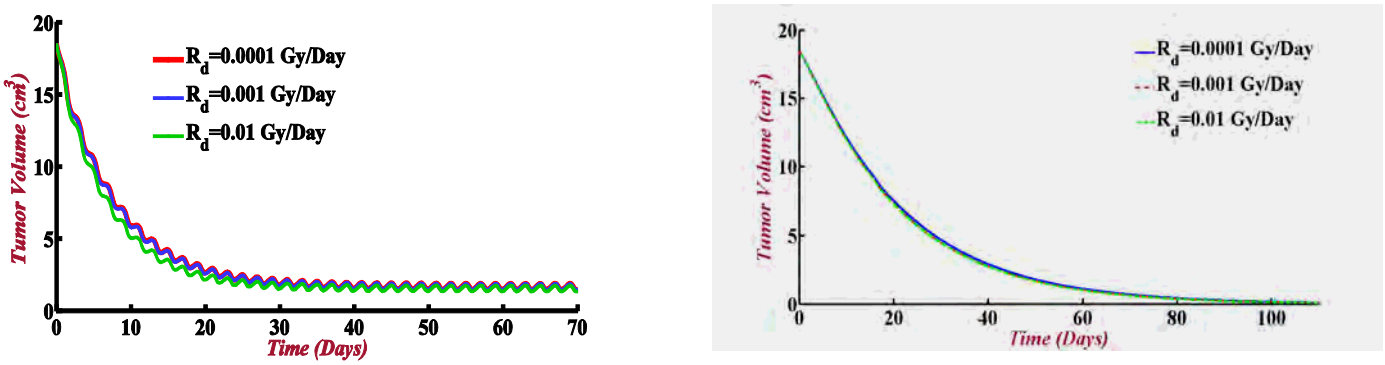

Fig. 11 Total tumor volume of (3.2) for constant $r = 1.5$ (left), and $r = \lambda = 0$ (right).

Figs 10, and 11 demonstrate that by increasing the radiation dose in each fraction (R_d), the tumor volume decreases and quickly converges to a particular volume. On the other hand, in Figure 10 (right), the tumor volume approaches zero if we maintain the nutrition rate $r = 0$. Additionally, by preserving the Gompertz growth and nutrition rate at zero for continuous dosing, the volume of tumors can be controlled to be zero.

Impact of the value of $\frac{\alpha}{\beta}$ to radiotherapy result

According to the model, the influential facts of quiescent cells on tumor radiotherapy include the initial volume, the transition probability of quiescent cells to other cells, and $\frac{\gamma}{\delta}$, which is the radiation sensitivity parameters. The model's application to clinical radiation may require all of the parameters. The radiation sensitivity of tumor cells is indicated by $\frac{\gamma}{\delta}$. In general, the linear action of the LQ model is of greater significance compared to the quadratic action as the $\frac{\gamma}{\delta}$ ratio increases. Under the same settings, the larger the $\frac{\gamma}{\delta}$ ratio, the flatter the tumor control curve is, and more fractional times or dosages are required. Because of the activity of quiescent cells in our model, the simulation results are also influenced by $\frac{\gamma_2}{\delta_2}$, the radiation sensitivity of quiescent cells. We may use the model to determine that the higher the ratio of $\frac{\gamma_2}{\delta_2}$, the worse the radiation effect.

Example 8. We consider Equation (3.2) with $= 0.005, \lambda = 0.75, r_{12} = r_{21} = 0.1, r_{13} = r_{23} = 0.05$. We take here $K = 1.2 + \cos(\pi t), \eta = 0.3, \gamma_1 = 1.5, \delta_1 = 0.125$, the radiotherapy dose $R_d = 0.01$ we take the ratio $\frac{\gamma_2}{\delta_2} = 4.12, 3, 7$.

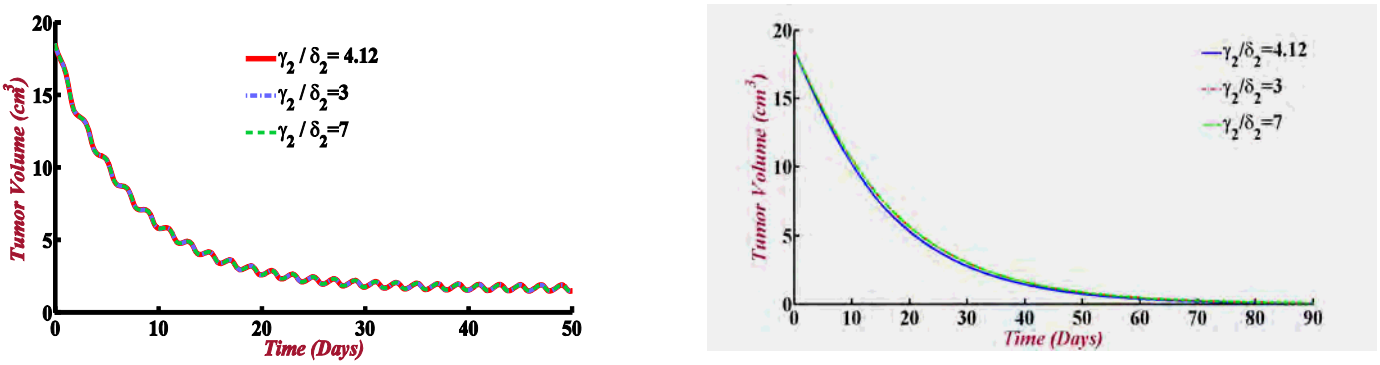

Fig. 12 Total tumor volume of (3.2) for constant $r = 1.5$ (left) and $r = \lambda = 0$ (right).

Fig. 12 represents the dynamics of the tumor volume for various ratios of $\frac{\gamma_2}{\delta_2}$ and a constant radiation dose.

For $r = \lambda = 0$, the volume of tumors can be maintained at a neutral level in Fig. 12 (right).

6 Summary and Concluding Remarks

In the radiation therapy model, two different divisions are available. One of them is a normal model focusing on the initiation and progression of cancer, while the remaining one is related to the interpretation of malignant cells and radiation particles. In the first model, the GM is considered a prominent mathematical model. The complex biological processes could be described comprehensively with this model, which helps create a new dimension of tumor research. Since the biomedical procedures are complex and have limited research conditions, a basic investigation of tumor characteristics could be done with this model. It is impossible to use all kinds of mathematical modeling from the clinical perspective without appropriate quantized model parameters. Scientists are trying rigorously to get solutions in this aspect so that mathematical modeling can be used in the clinical research of tumors. The interaction model tests with radiation particles and cancer cells began in the 1960s, using an output from the widely used LQ model. Recent studies show that broad mathematical modeling and the LQ model can be successfully coupled to predict the effect of radiation. This paper provides a 3-C tumor model to investigate the influence of the dormant cell. The simulation results reveal that the primary volume of the quiescent cell and the radiation sensitivity coefficient can influence radiation therapy. By integrating a more exact model and genuine model characteristics, the 3-C tumor model could be more useful in clinical settings. The investigations allow us to quantify the relationship between the indexes and our model parameters. Some patient-specific factors can be retrieved and fit to real-world biological data. This study is intended to open the way for more effective investigation of mathematical modeling in tumor radiation therapy.

Acknowledgments

The author, M. Kamrujjaman research, was partially supported by the University Grants Commission (UGC), and the University of Dhaka, Bangladesh. Conceptualization, MK and SIA; methodology, SA and SIA; software, SIA, MK and SA; validation, AAA and MAM; formal analysis, SIA and MK; investigation, SA and AAA; resources, MAM; data curation, SIA; original draft preparation, SIA and MK; review and editing, MK, AAA, and MAM; supervision, MK. All authors have read and agreed to the published version of the manuscript.

References

Adam JA 1996. Mathematical models of perivascular spheroid development and catastrophe theoretic description of rapid metastatic growth/tumor remission. Invastion and Metastasis, 16: 247-267

Alam M, Kamrujjaman M, Islam M. 2020b. Parameter sensitivity and qualitative analysis of dynamics of ovarian tumor growth model with treatment strategy. Journal of Applied Mathematics and Physics, 8.06: 941-955

Araujo RP, McElwain DLS. 2004c. A history of the study of solid tumor growth: The contribution of mathematical modelling. Bulletin of Mathematical Biology, 66: 1039-1091

Borkenstein K, Levegrün S, Peschke P. 2004a. Modeling and computer simulations of tumor growth and tumor response to radiotherapy. Radiaant Research, 162(1): 71-83

Bratus AS, Fimmel E, Kovalenko SY. 2014c. On assessing quality of therapy in non-linear distributed mathematical models for brain tumor growth dynamics. Mathematical Bioscience, 248: 88-96

Byrne HM. 1999a. The role of mathematics in solid tumour growth. Math Today, 35: 59-89

Cappuccio A. 2006. Cancer immunotherapy by interleukin-21: potential treatment strategies evaluated in a mathematical model. Cancer Research, 66(14): 7293-300

Carmeliet P and Jain RK. 2000. Angiogenesis in cancer and other diseases. Nature, 407: 249-257

Blagosklonny MV. 2004d. Antiangiogenic therapy and tumor progression. Cancer Cell, 5: 13-17

Chvetsov AV, Dong L, Palta JR, et al. 2009e. Tumor-volume simulation during radiotherapy for head-and-neck cancer using a four-level cell population model. International Journal of Radiation Oncology - Biology - Physics, 75: 595-602

Cooper GM, Hausman RE, & Hausman RE. 2007d. The Cell: A Molecular Approach. ASM Press, Washington DC, USA

Cristini V, Li X, Lowengrub JS, Wise SM. 2009a. Nonlinear simulations of solid tumor growth using a mixture model: invasion and branching. Journal of Mathematical Biology, 58(4-5): 723-763. doi:10.1007/s00285-008-0215-x.

Deisboeck TS, Stamatakos GS. 2010a. Editors. Multiscale Cancer Modeling. Chapman and Hall/CRC Mathematical and Computational Biology (Book 34). CRC Press, Boca Rayton, USA

Domijan M, Brown PE, Shulgin BV, et al. 2016c. PeTTSy: a computational tool for perturbation analysis of complex systems biology models. BMC Bioinform, 17(1): 124

Elisabet OP. 2015. Some Mathematical Models of Tumor Growth. Graduate Thesis

Enderling H, Chaplain MAJ, Anderson ARA, Vaidya JS. 2007b. A mathematical model of breast cancer development, local treatment and recurrence. Journal of Theoretical Biology, 246(2): 245-59

Ferlay J, Soerjomataram I, Dikshit R, et al. 2015a. Cancer incidence and mortality worldwide: sources, methods and major patterns in GLOBOCAN 2012. International Journal of Cancer, 136: E359-E386

Folkman J. 1972. Antiangiogenesis: new concept for therapy of solid tumors. Annals of Surgery, 175: 409416

Gao X, McDonald JT, Hlatky L, Enderling H. 2013a. Acute and fractionated irradiation differentially

modulate glioma stem cell division kinetics. Cancer Research, 73(5): 1481-1490

Hahnfeldt P, Panigrahy D, Folkman J, Hlatky L. 1999b. Tumor development under angiogenic signaling: a dynamical theory of tumor growth, treatment response, and postvascular dormancy. Cancer Research, 59(19): 4770-4775

Harting C, Peschke P, Borkenstein K, Karger CP. 2007c. Single-cell-based computer simulation of the oxygen-dependent tumour response to irradiation. Physics in Medicine & Biology, 52(16): 4775-4789. doi:10.1088/0031-9155/52/16/005

Hossine Z, Meghla AA, Kamrujjaman M. 2019a. A short review and the prediction of tumor growth based on numerical analysis. Advances in Research, 19.1: 1-10

Ira JI, et al. 2020a. Mathematical modelling of the dynamics of tumor growth and its optimal control. International Journal of Ground Sediment and Water, 11: 659-679

Jemal A, Bray F, Center MM, et al. 2011a. Global cancer statistics. CA: A Cancer Journal of Clinicians, 61: 69-90

Kamrujjaman M, Mahmud MS, Islam MS. 2021. Dynamics of a diffusive vaccination model with therapeutic impact and non-linear incidence in epidemiology. Journal of Biological Dynamics, 15(sup1): S105-S133

Kim Y, Magdalena AS, Othmer HG. 2007a. A hybrid model for tumor spheroid growth in vitro I: theoreical development and early results. Math Models and Methods in Applied Science, 17: 1773-1798

Kim Y, Stolarska MA, Othmer HG. 2011b. The role of the microenvironment in tumor growth and invasion. Progress in Biophysics and Molecular Biology, 106(2): 353-379. doi:10.1016/j.pbiomolbio.2011.06.006

Macklin P, Edgerton ME, Thompson AM, Cristini V. 2012a. Patient-calibrated agent based modelling of ductal carcinoma in situ (DCIS): from microscopic measurements to macroscopic predictions of clinical progression. Journal of Theoretical Biology, 301: 122-140

Marcu L, Bezak E. 2009c. Radiobiological modeling of interplay between accelerated repopulation and altered fractionation schedules in head and neck cancer. Journal of Medical Physics, 34(4): 206

Marino S, Hogue IB, Ray CJ, et al. 2008b. Kirschner. A methodology for performing global uncertainty and sensitivity analysis in systems biology. Journal of Theoretical Biology, 254: 178-196

Masahiro M, Seishin T, Hiroyuki D, et al. 2012c. A mathematical study to select fractionation regimen based on physical dose distribution and the linear quadratic model. International Journal of Radiation Oncology - Biology - Physics, 84: 829-833

Matthias G, Rainer JK, Michael A, et al. 2013b. Applicability of the linear quadratic formalism for modeling local tumor control probability in high dose per fraction stereotactic body radiotherapy for early stage non-small cell lung cancer. Radiotherapy and Oncology, 109: 13-20

Michor F, Iwasa Y, Nowak MA. 2004b. Dynamics of cancer progression. Nature Reviews Cancer, 4: 197-205

Nawrocki S, Zubik-Kowal B. 2014b. Clinical study and numerical simulation of brain cancer dynamics under radiotherapy. Communications in Nonlinear Science and Numerical Simulation. doi:10.1016/j.cnsns.2014.08.001

Nazila B, Lotfi MM. 2016a. A multi-objective multi-drug model for cancer chemotherapy treatment planning: a cost-effective approach to designing clinical trials. Computers and Chemical Engineering, 87: 226-233

Perez-Garcia VM, Bogdanska M, Martinez-Gonzalez A, Belmonte-Beitia J, Schucht P, Perez-Romasanta LA. 2014a. Delayeffects in the response of low-grade gliomas to radiotherapy: a mathematical model and its therapeutical implications. Mathematical Medicine and Biology. doi:10.1093/imammb/dqu009

Powathil GG, Gordon KE, Hill LA, Chaplain MAJ. 2012b. Modelling the effects of cell cycle heterogeneity on the response of a solid tumor to chemotherapy biological insights from a hybrid multiscale cellular automaton model. Journal of Theoretical Biology, 308(C): 1-19

Rockne R, Alvord E, Rockhill J, Swanson K. 2009d. A mathematical model for brain tumor response to radiation therapy. Journal of Mathematical Biology, 58(4): 561-578. doi:10.1007/s00285-0080219-6

Rockne R, Rockhill JK, Mrugala M, Spence AM, Kalet I, Hendrickson K, et al. 2010b. Predicting the efficacy of radiotherapy in individual glioblastoma patients in vivo: a mathematical modeling approach. Physics in Medicine and Biology, 55(12): 3271-3285

Titz B, Jeraj R. 2008a. An imaging-based tumour growth and treatment response model: investigating the effect of tumour oxygenation on radiation therapy response. Physics in Medicine and Biology, 53(17): 4471-4788

Wang CH, Rockhill JK, Mrugala M, Peacock DL, Lai A, Jusenius K, et al. 2009b. Prognostic significance of growth kinetics in newly diagnosed glioblastomas revealed by combining serial imaging with a novel biomathematical model. Cancer Research, 69(23): 9133-9140

Wensong H, Gangqing Z. 2019b. Simulation analysis for tumor radiotherapy based on three-component mathematical model. Journal of Applied Clinical Medical Physics, 20(3): 22-26

Yoichi W, Erik LD, Kevin ZL, et al. 2016b. A mathematical model of tumor growth and its response to single irradiation. Theoretical Biology and Medical Modelling, 13: 6